

Diffusing Probe Measurements of Polystyrene Latex Particles in Polyelectrolyte Solutions: Deviations from Stokes–Einstein Behavior

Dave E. Dunstan^{*,†} and Jason Stokes

CRC for Bioproducts, Department of Chemical Engineering, University of Melbourne, Parkville 3052, Australia

Received June 15, 1998; Revised Manuscript Received September 24, 1999

ABSTRACT: The diffusion coefficients of polystyrene latex spheres in both Newtonian and elastic liquids have been measured using dynamic light scattering. The diffusion coefficients of the latex particles measured in glycerol/water (Newtonian) solutions obey Stokes–Einstein behavior over a range of solvent viscosity and temperature. Two apparent diffusion coefficients for the particles are measured in viscoelastic polyacrylamide solutions and are designated D_{fast} and D_{slow} . The apparent fast diffusion coefficients measured in the polyacrylamide solutions show an increase to a maximum, above that measured in the solvent water, with increasing polyacrylamide concentration. The apparent fast diffusion coefficient is seen to increase to twice that measured in the water solvent. At higher polyacrylamide concentrations the observed D_{fast} values decrease below the value obtained in the solvent water. D_{fast} increases with the scattering vector (q) while D_{slow} is independent of q .

Introduction

The use of colloidal particles as probes in polymer solutions and gels is not new. A significant number of studies have measured the diffusion of colloidal probes in a wide variety of polymer solutions in both aqueous and nonaqueous solvents.^{1–18} The probe particles are thought to sense their local environment in the polymer or polyelectrolyte solution and thus probe the internal structure of the solution. Our interest in these measurements has arisen from the nonperturbative nature of the measurements in examining polyelectrolyte solutions and gels. The measured diffusion coefficient of the probe particles is generally interpreted as a microviscosity using the Stokes–Einstein equation. The microviscosity is simply the viscosity of the particle environment in the polymer or polyelectrolyte solution which has been shown to deviate from the macroscopic viscosity in a number of cases. For Newtonian solvents the micro- and macroviscosities generally appear to be the same while for polymer and polyelectrolyte solutions significant differences have been observed. In polyelectrolyte solutions the solution viscosity may not be uniform on the length scales of the diffusive fluctuations of the particles, and differences between the micro- and macroviscosities may be measured to yield structural information pertaining to the polymer/polyelectrolyte solution.

The Stokes–Einstein equation is used to relate the measured diffusion coefficients to the solvent viscosity

$$D = kT/6\pi\eta R_h \quad (1)$$

where D is the diffusion coefficient, k Boltzmann's constant, T the absolute temperature, η the solution viscosity, and R_h the hydrodynamic radius of the particle. The Stokes–Einstein relation may be used to interpret the measured diffusivity as a viscosity. Prior work has used the normalization of the viscosity and diffusivity by the product $D\eta/D_0\eta_0$ where D_0 and η_0 are the diffusivity of the probe in the solvent and the solvent

viscosity, respectively. Positive and negative deviations from Stokes–Einstein behavior are defined as the product being greater than or less than 1, respectively. The number of papers in the area is significant and are well summarized in the work of Won et al.¹ Both positive and negative deviations are observed in a number of solvents and probe/polymer mixtures. A significant number of papers show adherence to S–E behavior such that $D\eta/D_0\eta_0 = 1$. A positive deviation from S–E behavior corresponds to a microviscosity which is less than the macroscopic viscosity of the solution. To avoid confusion, we have not normalized the diffusion coefficients measured in this work, since the absolute values are significant as will be shown later. The viscosities of the polymer solutions are often not Newtonian, and therefore, the normalization used above is often not valid. The shear rate of the measurement must be specified while the shear rate at the particle surface is not known. Many of the prior works have relied on capillary viscometry for the measurement of viscosity without specification of the shear rate. Given that most polymer or polyelectrolyte solutions show viscoelastic behavior, this normalization procedure may be prone to error. However, there currently exists no method, other than capillary viscometry, known to the authors for measuring the viscosity–shear rate behavior of truly dilute polymer and polyelectrolyte solutions.

This study reports the measurement of the diffusion of latex tracer particles in Newtonian glycerol/water mixtures and in highly elastic polyacrylamide solutions (Separan AP30). The observed increase in the measured apparent fast diffusion coefficients in the polyacrylamide solutions is discussed with reference to the viscoelastic nature of these solutions.

Experimental Section

Triply distilled water was used in all experiments. AR glycerol obtained from BDH was used after centrifugation to remove all dust.

The latices used were obtained from Interfacial Dynamics Corporation and used without further purification. Both sulfate latices of 0.2 μm diameter and amidine latices of 0.068

[†] E-mail: d.dunstan@chemeng.unimelb.edu.au.

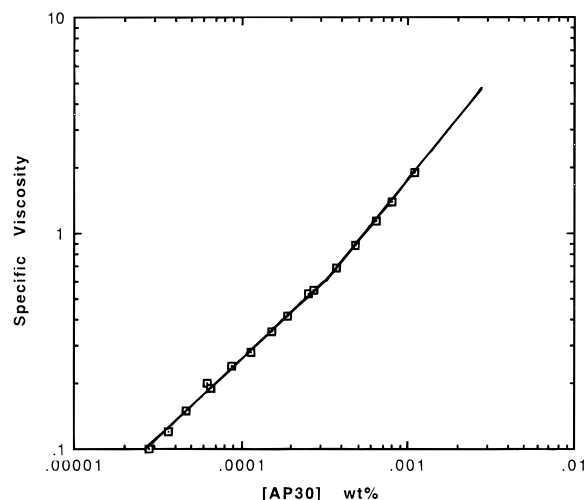


Figure 1. Relative viscosity vs AP30 concentration measured using an Ubbelohde capillary viscometer. Shear rates were as high as 1000 s^{-1} . The critical overlap concentration was determined as 0.0003 wt % from the data as described in the text.

μm diameter. These lattices show both negative and positive surface charges, respectively. Surface charge densities of -0.8 and $+4.8 \mu\text{C}/\text{cm}^2$ for the sulfate and amidine lattices were obtained from conductimetric titration by IDC. Sizes obtained from light scattering were 0.20 and $0.067 \mu\text{m}$ average diameter by volume which are in agreement with the electron microscope sizes of 0.20 and $0.068 \mu\text{m}$ also determined by Interfacial Dynamics Corporation.

The polyacrylamide was a Separan AP30 sample obtained from Dow Chemical Company with a weight-average molecular weight of 3.1×10^6 with a polydispersity of 1.07 as measured using GPC/MALLS. The manufacturer states that the AP30 has a 30% degree of ionization and is thus an anionic polyelectrolyte in the pH range 6.8 – 10.4 . The measured pH of the 1% AP30 solution was 10.4 which decreased upon dilution in water over the range of the measurements. The polyacrylamide was dissolved in water at 1 wt % and centrifuged to remove any dust as measured by light scattering. This solution was then diluted to the measured concentration with water and a small aliquot of the tracer particles. The aliquot of tracer particles was adjusted such that the scattered intensity was as low as possible to ensure that no particle/particle interactions nor multiple scattering occurred, to obtain diffusion coefficients for truly dilute solutions. The critical overlap concentration for the AP30 was difficult to measure accurately as the shear rates of the capillary viscometers were quite high. The measured intrinsic viscosity in water for the AP30 was 450 L/g . The data shown in Figure 1 is for shear rates as high as 1000 s^{-1} and shows C^* to be approximately $0.0003 \text{ wt } \%$. This figure should be treated with caution due to the high shear rate of the measurement. The observed behavior shows only a slight discontinuity at the apparent C^* . C^* was obtained by extrapolation of the limiting slopes and taking the concentration at the intersection of the two lines. Plotting the relative viscosity vs concentration (not shown) yielded a curved line which gave $0.0003 \text{ wt } \%$ as the intersection of the line drawn through the limiting slopes.

Ubbelohde capillary viscometers were used to measure the viscosities of the glycerol/water solutions and in the attempt to measure the critical overlap concentration of the AP30 solutions. A Weissenberg controlled shear rate instrument was used for the measurement of viscosity shear rate and normal stress for the polyacrylamide solutions. Viscosity-shear rate and first normal stress difference were measured at 1 wt % AP30. Measurements at lower concentrations are difficult as the experimental sensitivity of the rheometer is inadequate at low viscosities. The cone and plate geometry was used for the controlled shear measurements with a 6 cm diameter cone with a 2° angle.

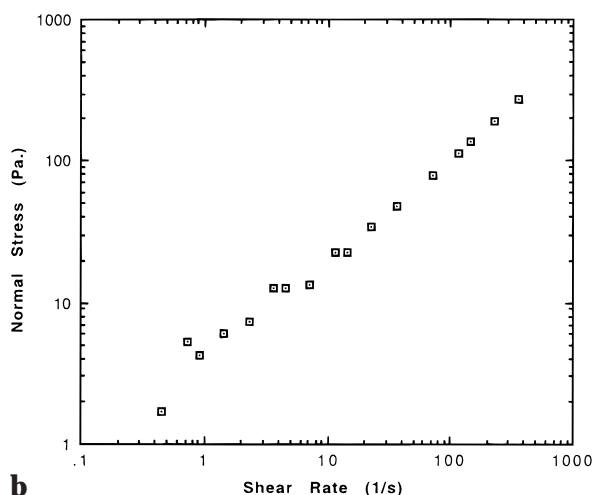
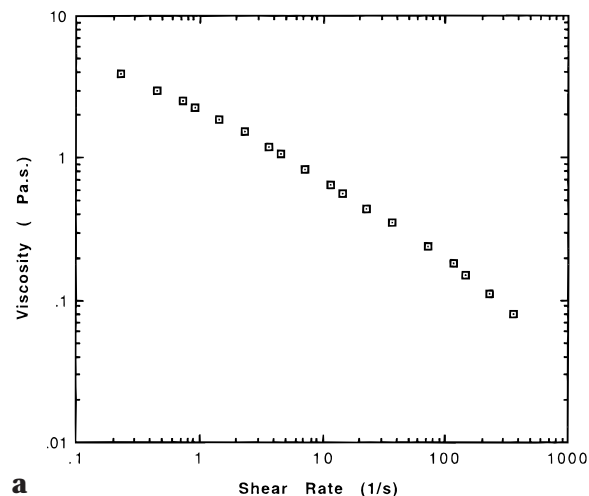


Figure 2. (a) Viscosity vs shear rate for the 0.1 wt % polyacrylamide solution. (b) The first normal stress difference vs shear rate for the 0.1 wt % polyacrylamide solution.

Parts a and b of Figure 2 show the rheological data obtained for the AP30 used in this study. Significant shear thinning behavior is observed for this polymer solution combined with the first normal stress difference increasing with shear rate as is expected for viscoelastic fluids.^{19,20} The viscosity-shear rate and the first normal stress difference are shown as a function of shear rate for a 1 wt % AP30 solution. The observed behavior is typical for high molecular weight polymer and polyelectrolyte solutions at a low electrolyte concentration and is typical of highly elastic fluids such as high molecular weight polyacrylamides in water.²⁰

Dynamic light scattering was performed using a Malvern 4700 apparatus with a 10 mW Ar^+ ion laser at 488 nm . Measurements were made at an angle of 90° and a temperature of 25°C , unless otherwise stated.

The dynamic light scattering experiment involves measurement of rapid time fluctuations in the intensity of the scattered light. The intensity fluctuations arise from the translation diffusion of the ensemble of particles in space which interfere due to phase shifts associated with the random particle motions. The time correlation function (TCF) of the scattered intensity is given by

$$G_2(t) = \langle I(0) I(t) \rangle \quad (2)$$

where I is the measured intensity at time t and the brackets represent the time average. The second-order autocorrelation function is then defined as

$$g_2(t) = \langle I(t) I(t + \tau) \rangle / \langle I(t) \rangle^2 \quad (3)$$

where τ is the delay time.

The experimental autocorrelation function is normalized by the experimental baseline intensity A to give the theoretical field autocorrelation function defined as

$$g_2(\tau) = A + B \langle g_1(\tau) \rangle^2 \quad (4)$$

where A and B are optical constants for the measuring system.

The data are commonly analyzed by fitting a normalized second-order autocorrelation function.²¹

$$g_1(\tau) = \{a_1 \exp(-\mathbf{q}^2 D_{\text{fast}} \tau) + a_2 \exp(-\mathbf{q}^2 D_{\text{slow}} \tau)\}^2 + 1 \quad (5)$$

a_1 and a_2 are amplitudes of the intensities from the scattering population with diffusion coefficients D_{fast} and D_{slow} respectively.

The apparent diffusion coefficients are interpreted from the measured relaxation times of the autocorrelation function using the relationship

$$\Gamma = D\mathbf{q}^2 \quad (6)$$

where Γ is the relaxation time and \mathbf{q} the scattering vector defined as

$$\mathbf{q} = (4\pi n/\lambda) \sin(\theta/2) \quad (7)$$

λ is the wavelength of the light, n the refractive index, and θ the scattering angle.

The time correlation functions were analyzed using the CONTIN algorithm supplied with the instrument.²² This algorithm fits a multiexponential curve to the time correlation function such that the residuals are minimized over the time range measured.

Second-order fits were obtained for the probe particles in the polyelectrolyte solutions yielding two apparent diffusion coefficients D_{fast} and D_{slow} . In all cases the residuals were random and less than 0.005 of the normalized correlation function. Prior studies have also observed a double exponential decay of the autocorrelation function for probe particles in high molecular weight polymer solutions.¹⁴ Both cumulants and CONTIN analysis of the data and the relative merits of the fitting procedures have been discussed in the prior works.^{14,16,18} Mustafa and Russo interpret two diffusion coefficients from their data for probe particles in hydroxypropylcellulose and conclude that to constrain the fit to a single exponential, namely a cumulants fit, may be misleading.¹⁴

Results and Discussion

Figure 3 shows the measured diffusion coefficients vs viscosity for the 0.2 μm latex particles in glycerol/water solutions. Within experimental error, the Stokes–Einstein equation is obeyed over a range of Newtonian solvent viscosities. The measured diffusion coefficient varies inversely with the viscosity for the Newtonian glycerol/water solutions.

Figure 4 shows the measured diffusion coefficients of the particle vs temperature divided by the viscosity for the 0.2 μm latex particles in water over the range of 10–70 °C. Linearity is observed with a slope of $k/6\pi R_h$. Interestingly, no apparent surface hairiness effects are observed where polyelectrolyte surface groups produced in the particle polymerization reaction change the hydrodynamic radius of the particle with temperature.²³ The data of Figures 3 and 4 show that the Stokes–Einstein equation is obeyed over a range of temperatures and viscosities for Newtonian solvents for the 0.2 μm particles. These data is consistent with that observed by Phillies for latex particles in glycerol/water

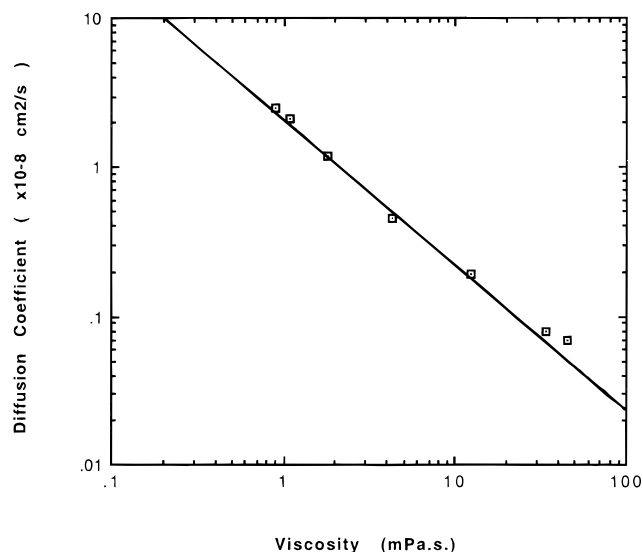


Figure 3. Measured diffusion coefficient vs viscosity in glycerol water solutions for the 0.2 μm particles.

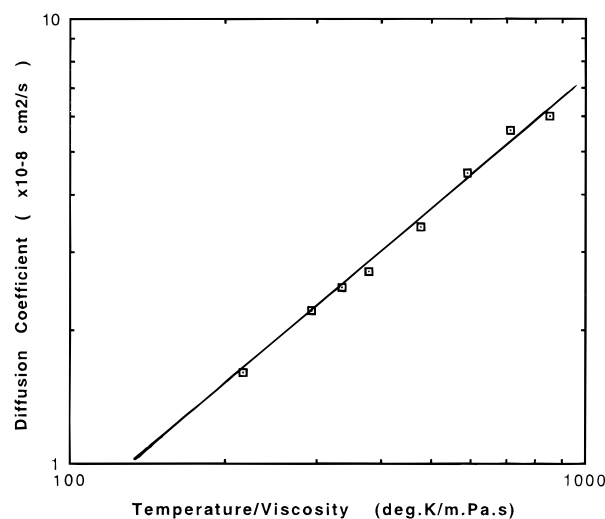


Figure 4. Measured diffusion coefficient vs temperature/viscosity for the 0.2 μm particles in water. The slope of the curve is equal to $k/6\pi R_h$. The temperature range was 10–70 °C. Viscosities were taken from the literature: *CRC Handbook of Physics and Chemistry*, Vol. 74.

solutions where D is shown to scale with T/η at several glycerol/water ratios.¹⁵

The measured diffusion coefficient of the AP30 molecules at 1 wt % is $4.5 \times 10^{-7} \text{ cm}^2/\text{s}$ to yield a hydrodynamic radius of 3 nm when normalized for the low shear viscosity of the AP30 solution. This value should be treated with some caution as the polyelectrolyte molecules in solution interact at this concentration. The measured value of D for the polyelectrolyte is approximately 1 order of magnitude greater than the values observed for the latex probe particles as shown in Figure 3. The refractive index difference between the water and the polyacrylamide did not allow the diffusion coefficient for solutions at lower concentrations than approximately 1 wt % to be measured. However at this, the highest polyelectrolyte concentration used, the intensities of the scattering from the particles were approximately 200 times that of the polymer. The measured diffusion coefficients are therefore attributable to the particles and are not a direct measure of the polyelectrolyte diffusion.

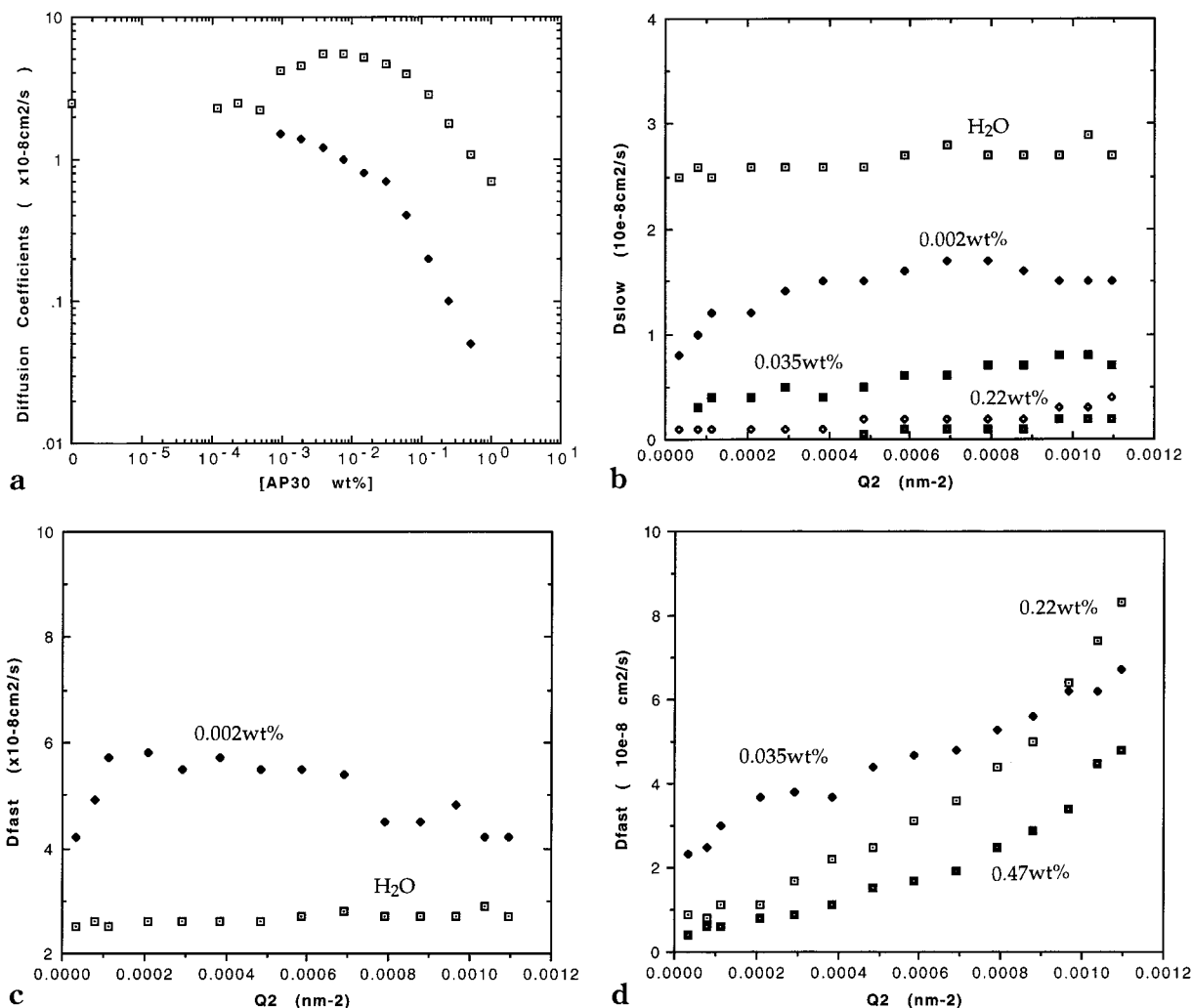


Figure 5. (a) Measured diffusion coefficients vs concentration of polyacrylamide for the 0.2 μ m sulfate latices. Two diffusion coefficients were obtained from the data which are designated D_{fast} and D_{slow} . The point on the left-hand vertical axis at 2.5 is for pure water. (b) Measured D_{slow} values vs q^2 for the 0.2 μ m particles in water and 0.002, 0.035, 0.22, and 0.47 wt % AP30. (c) Measured D_{fast} values vs q^2 for the 0.2 μ m particles in water and 0.002 wt % AP30. (d) Measured D_{fast} values vs q^2 for the 0.2 μ m particles in 0.035, 0.22, and 0.47 wt % AP30.

The measured diffusion coefficients, both D_{fast} and D_{slow} , at a scattering angle of 90° for the 0.2 μ m particles in a range of AP30 concentrations are shown in Figure 5a. Two diffusion coefficients are interpreted from the autocorrelation function at each concentration above approximately 0.001 wt %. Below this value a single number is obtained as the resolving power of the algorithm is limited. One broad distribution of diffusion coefficients is interpreted from the autocorrelation function at lower polyacrylamide concentrations. The diffusion coefficient for the higher value, D_{fast} , increases to approximately twice that measured in the solvent at AP30 concentrations of order 0.005 wt %. The lower value, D_{slow} , decreases with increasing AP30 concentration, while still being larger than expected from the low shear macroscopic viscosity of the AP30 solutions. Interestingly, the measured critical overlap concentration of 0.0003 wt % is well below the concentration where the maximum in the apparent D_{fast} is observed and the concentration at which the discontinuity of the slope of the D_{slow} vs AP30 concentration occurs. The splitting of the measured diffusion into two diffusion coefficients occurs at concentrations greater than 0.0003 wt %, the measured value of C^* , as seen in Figure 5a.

The angular dependence of the apparent diffusion coefficients is shown in Figures 5b through to 5d. The D_{slow} values measured over a range of concentrations show no angular dependence from 20 to 150° as seen in Figure 5b. The corresponding q^2 range is 3×10^{-5} to 1.1×10^{-3} nm⁻². This indicates that the slow mode is a truly diffusional process. The D_{fast} values show an angular dependence which varies with the AP30 concentration. As shown in Figure 5c the measured diffusion coefficient is independent of q^2 in the solvent water. At 0.002 wt % AP30, the D_{fast} shows a maxima with q^2 while at higher concentrations D_{fast} increases significantly with q^2 as shown in parts c and d of Figure 5. The D_{fast} values obtained from extrapolation of the data to $q^2 = 0$ show the same trend as measured at a scattering angle of 90°. (See Figure 5a.) The D_{fast} values show q^2 dependence at concentrations above C^* . Interestingly, the apparent fast diffusion coefficients at higher concentrations increase with q^2 where the distances probed are the smallest. This is consistent with the idea of anisotropic caging by the AP30 where the probe particles are confined by the surrounding polyelectrolyte. The constrained motion of the particles is more rapid on shorter length scales and is more rapid

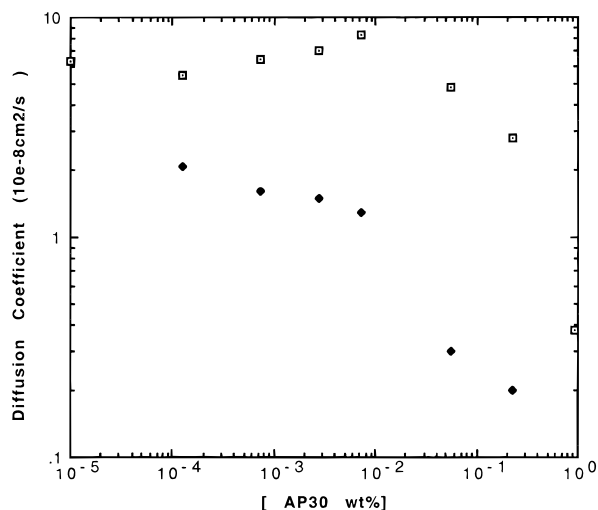


Figure 6. Measured diffusion coefficients vs concentration for the 0.068 μm diameter amidine latex particles in AP30. The point shown on the vertical axis is for pure water.

than in the pure solvent indicating the presence of either a macroscopic fluctuation of the AP30 solution or an elastic fluctuation. D_{fast} rises rapidly at shorter length scales ($1/q$) for the higher AP30 concentrations. Plotting D_{fast} vs $1/q$ (not shown) shows D_{fast} rising very rapidly and asymptotes toward 30 nm for all AP30 concentrations.

The slower diffusion coefficient (see Figure 5a) is also noncompliant with the S–E equation.²⁰ Assuming the viscosities shown in Figure 1 are simple Newtonian viscosities yields values of D_{slow} which are larger than those observed from the data of Figure 5a. The discontinuity in the slope of the curve of D_{slow} vs AP30 concentration may correspond to the critical overlap concentration in the truly unperturbed solution. C^* was measured at a high shear rate where alignment of the polyelectrolyte in the shear field will occur, giving rise to less interaction than in the unsheared state. The high shear data should therefore yield an overestimate of the true equilibrium value of C^* which exacerbates the difference between the two values. The measured D_{slow} values are independent of q^2 as shown in Figure 5b. This behavior is typical of diffusion in a viscous solvent as was observed in the glycerol solutions. A slow diffusion process in polymer solutions has been observed by Djabourov et al. in gelatin gels using diffusing probes and has been attributed to the restriction of the available diffusion modes.²⁴ Mustafa and Russo have also observed two apparent diffusion coefficients for measurements of latex tracer particles in high molecular weight polymers.¹⁴

The measured diffusion coefficients for the 0.068 μm diameter latex vs AP30 concentration are shown in Figure 6. In a manner similar to that observed for the 0.2 μm particles, the fast diffusion coefficient increases with increasing AP30 concentration to a maximum to then decrease at higher concentrations. The relative increase in D for the smaller latex particles is not as large as is observed for the 0.2 μm particles. The diffusion coefficient increases by a factor of 1.5 for the 0.068 μm particles compared to D_{fast} reaching a maximum at twice that measured in the solvent for the 0.2 μm particles. The dependence of the apparent diffusion coefficients on q^2 has not been measured for the amidine latices. Furthermore, the measured diffusion coefficients are greater than those of the solvent for both positive

(0.068 μm) and negatively charged (0.2 μm) particles. Adsorption of the AP30 to the amidine latex would be expected to occur due to electrostatic interactions. Adsorption of the polymer to the particles would increase the hydrodynamic radius and thus reduce the measured diffusion coefficient.

The observation that the measured diffusion coefficients in the polyacrylamide solutions are larger than in the solvent is significant. Mustafa and Russo and Ullmann et al. have also observed a fast diffusional mode for latex tracers in polymer solutions.^{14,17} The diffusion derives from a balance between the thermal and viscous forces acting on the particles. The resultant Brownian motion is described in eq 1 for a Newtonian fluid. Stochastic thermal fluctuations in the solvent accelerate the particle and at equilibrium are balanced by the hydrodynamic drag forces.²⁵ The random nature of the thermal fluctuations results in a random trajectory of the particle through solution. Several factors may effect this motion in polymer or polyelectrolyte solutions apart from the change in the solvent viscosity, as will be discussed below.

A significant body of work by a number of researchers exists in the literature showing both positive and negative deviations from Stokes–Einstein behavior.^{1–18} The generally accepted method for displaying the data is to normalize the diffusion coefficients by the solvent viscosity as is discussed in the Introduction. In many cases the viscosity is measured by the use of capillary viscometers where the shear rate is not quoted. As is demonstrated in Figure 2a, the viscosity of polyelectrolyte solutions is not a single number. Furthermore, the normalization of D by the viscosity may hide aspects of the behavior which are important. The work presented here is of interest in that the increase in diffusion coefficient with polyelectrolyte concentration, where the absolute value of D_{fast} increases, is difficult to interpret physically. Other workers have however observed increases in the diffusion coefficients of latex tracers¹⁷ and ions in polyelectrolyte (AP30) solutions measured using a capillary method.²⁶ Ott and co-workers have also measured so-called hyperdiffusivity in micellar solutions.²⁷ Elasticity is hypothesized as the reason for the increase diffusivity observed in the prior works although no clear mechanism is elucidated.

The previously observed deviations from S–E behavior may be partially understood using the following arguments. The polymer may be depleted from the interfacial region resulting in the particle experiencing a viscosity which is lower than that observed for the bulk solution.²⁸ This behavior results in positive deviations from S–E behavior. However, the resultant diffusion may not increase above that observed in the pure solvent as is observed in this work for the polyacrylamide solutions. The polyelectrolyte may adsorb to the particle surface to increase the hydrodynamic size and thus decrease the diffusion coefficient resulting in negative deviations from S–E behavior. Polymer adsorption results in a reduced diffusivity while depletion effects may result in diffusion coefficients which would reach the solvent value at most. Neither depletion nor adsorption effects account for the behavior observed for the probe particles in the AP30 solutions. Interestingly, the early work of Phillies et al. for poly(acrylic acid) solutions and shows negative deviations from S–E behavior for the systems measured.¹³

The effect of elasticity is not considered in the derivation of the Stokes–Einstein equation where the solvent is considered to be Newtonian with a “nonslip” boundary condition at the particle surface.²⁵ Development of a theory describing the viscous drag on a sphere for elastic fluids requires sophisticated modeling and is beyond the theoretical capabilities of the authors. The effects of elasticity have been modeled using a drag reduction model where the Stokes drag is modified in a linear manner in elastic fluids.²⁶ Other workers have suggested a more complex relationship between the elasticity and viscosity in an attempt to understand the effects of elasticity on the diffusion of small ions in solution.²⁹ While the drag reduction effect is a surface phenomena, the mechanism by which the diffusion of ions and colloidal particles is increased is difficult to envisage.

Polyacrylamides in solution are also known to be drag reducing agents where the resistance to flow past surfaces is reduced.²⁵ The physical reasons for this phenomenon are not fully understood and may be similar to the mechanisms responsible for the observed increase in diffusivity of the probe particles. The larger particles show a greater increase in diffusivity consistent with lowered Stokes drag on the particles. This interpretation would involve the relaxation of the nonslip boundary condition at the particle surface leading to an increased diffusivity.²⁵

The elasticity of the AP30 solutions, as shown in parts a and b of Figure 2, may contribute to the diffusion of the particles through elastic storage of the thermal energy leading to an increased driving force for the particle motion. The normal stress and viscoelastic behavior is thought to derive from the deformation and orientation of the polymer molecules in shear fields. Recent experiments have indicated that viscoelastic behavior arises from the orientation of the prolate random polymer in the flow field.³¹ The normal stress is then an entropic force which arises from the randomization of the aligned polymer/polyelectrolyte molecules. The probe particles may sense a random elastic fluctuation in a manner similar to classical Brownian motion. A similar mechanism could account for the hyperdiffusivity observed by Ott et al.²⁷ in solutions of rodlike micelles.

Two diffusional modes have been predicted and measured in polymer solutions above the critical overlap concentration.^{32–35} These modes have been attributed to viscous and elastic fluctuations within the concentrated solution.³² The probe particles may therefore be sensing the elastic and viscous fluctuations in the concentrated polyelectrolyte solution. The measured D_{fast} and D_{slow} may therefore be attributed to the elastic and viscous fluctuations respectively in the polyelectrolyte solution at concentrations above C^* .

Conclusions

The Stokes–Einstein equation is obeyed for colloidal particles over a range of Newtonian solvent viscosities and temperatures. Measured diffusion coefficients are greater than those in water at finite polyacrylamide concentrations where a maximum with concentration is observed. This behavior is not fully understood and is postulated as due to either the elasticity of the polyacrylamide solutions where an elastic fluctuation is present or to a caged local motion of the probe particles. The measured D_{fast} increases with the scat-

tering vector at higher AP30 concentrations. Further work to quantify the effects of elasticity on D_{fast} is intended.

Acknowledgment. D.E.D. would like to acknowledge the support of the CRC for Industrial Plant Biopolymers during this work. J.S. would like to acknowledge the Commonwealth of Australia for financial assistance through an Australian Postgraduate Award.

References and Notes

- (1) Won, J.; Onyenemezu, C.; Miller, W. G.; Lodge, T. P. *Macromolecules* **1994**, *27*, 7389–7396.
- (2) Gold, D.; Onyenemezu, C.; Miller, W. G. *Macromolecules* **1996**, *29*, 5700–5709.
- (3) Wheeler, L. M.; Lodge, T. P. *Macromolecules* **1989**, *22*, 3399–3408.
- (4) Phillies, G. D. J.; Gong, J.; Li, L.; Rau, A.; Yu, L.-P.; Rollings, J. J. *Phys. Chem.* **1989**, *93*, 6219–6223.
- (5) Brown, W.; Rymden, R. *Macromolecules* **1988**, *21*, 840–846.
- (6) Furukawa, R.; Arauz-Lara, J. L.; Ware, B. R. *Macromolecules* **1991**, *24*, 599–605.
- (7) Onyenemezu, C. N.; Gold, D.; Roman, M.; Miller, W. G. *Macromolecules* **1993**, *26*, 3833–3857.
- (8) Gold, D.; Onyenemezu, C.; Miller, W. G. *Macromolecules* **1996**, *29*, 5710–5716.
- (9) Phillies, G. D. J.; Richardson, C.; Quinlan, C. A.; Ren, S. Z. *Macromolecules* **1993**, *26*, 6849–6858.
- (10) Phillies, G. D. J.; Lacroix, M.; Yambert, J. J. *Phys. Chem.* **1997**, *101*, 5124–5130.
- (11) Phillies, G. D. J.; Lin, T.-H. *J. Colloid Interface Sci.* **1984**, *100*, 82–95.
- (12) De Smedt, S. C.; Lauwers, A.; Demeester, J.; Engleborghs, Y.; De Mey, G.; Du, M. *Macromolecules* **1994**, *27*, 141–146.
- (13) Lin, T.-H.; Phillies, G. D. J. *Macromolecules* **1984**, *17*, 1686–1691.
- (14) Mustafa, M.; Russo, P. S. *J. Colloid Interface Sci.* **1989**, *129*, 240–253.
- (15) Phillies, G. D. J. *J. Phys. Chem.* **1981**, *85*, 2838–2843.
- (16) Tracy, M. A.; Pecora, R. *Macromolecules* **1992**, *25*, 337–349.
- (17) Ullmann, G. S.; Ullmann, K.; Lindner, R. M.; Phillies, G. D. J. *J. Phys. Chem.* **1985**, *89*, 692–700.
- (18) Phillies, G. D. J.; Malone, C.; Ullmann, K.; Ullmann, G. S.; Rollings, J.; Yu, L.-P. *Macromolecules* **1987**, *20*, 2280–2289.
- (19) Tam, K. C.; Tiu, C. *J. Rheol.* **1989**, *33*, 257–.
- (20) Ferry, J. D. *Viscoelastic Properties of Polymers*; Wiley: New York, 1980.
- (21) Southwick, J. G.; Jamieson, A. M.; Blackwell, J. *Macromolecules* **1981**, *14*, 1728–1732.
- (22) Provencher, S. W. *Comput. Phys. Commun.* **1982**, *27*, 229–238.
- (23) Chow, R. S.; Takamura, K. J. *J. Colloid Interface Sci.* **1988**, *125*, 226–232.
- (24) Djabourov, M.; Grillon, Y.; Leblond, J. *Polym. Gels Networks* **1995**, *3*, 407–428.
- (25) Russel, W. B.; Saville, D. A.; Schowalter, W. R. *Colloidal Dispersions*; Cambridge University Press: New York, 1989.
- (26) Wickramasinghe, S. R.; Boger, D. V.; Pratt, H. R. C.; Stevens, G. W. *Chem. Eng. Sci.* **1991**, *46*, 641–650.
- (27) Ott, A.; Bouchaud, J. P.; Langevin, D.; Urbach, W. *Phys. Rev. Lett.* **1990**, *65*, 2201–2205.
- (28) Napper, D. H. *Polymeric Stabilisation of Colloidal Dispersions*; Academic Press: New York, 1983.
- (29) Leslie, F. M.; Tanner, R. I. *Q. J. Mech. Appl. Math.* **1961**, *14*, 36–41.
- (30) Volk, H.; Freidrich, R. E. Polyacrylamide. Chapter 16 in *Handbook of Water Soluble Gums and Resins*; Davidson, R. L., Ed.; McGraw-Hill: New York, 1980.
- (31) Gason, S. J.; Dunstan, D. E.; Smith, T. A.; Chan, D. Y. C.; White, L. R.; Boger, D. V. *J. Phys. Chem.* **1997**, *101*, 7732–7735.
- (32) Tanaka, T.; Hocker, L. O.; Benedek, G. B. *J. Chem. Phys.* **1973**, *59*, 5151–5159.
- (33) Brochard, F.; de Gennes, P.-G. *Macromolecules* **1977**, *10*, 1157–1161.
- (34) Adam, M.; Delsanti, M. *Macromolecules* **1985**, *18*, 1760–1770.
- (35) Adam, M.; Delsanti, M. *Macromolecules* **1977**, *10*, 1229–1237.